Geomechanics and Engineering, *Vol. 15, No. 1 (2018) 621-630*
DOI: https://doi.org/10.12989/gae.2018.15.1.621

Catastrophe analysis of active-passive mechanisms for shallow tunnels with settlement

X.L. Yang* and H.Y. Wang[a]

School of Civil Engineering, Central South University, Hunan 410075, China

(Received April 14, 2017, Revised October 19, 2017, Accepted November 8, 2017)

Abstract. In the note a comprehensive and optimal passive-active mode for describing the limit failure of circular shallow tunnel with settlement is put forward to predict the catastrophic stability during the geotechnical construction. Since the surrounding soil mass around tunnel roof is not homogeneous, with tools of variation calculus, several different curve functions which depict several failure shapes in different soil layers are obtained using virtual work formulae. By making reference to the simple-form of Power-law failure criteria based on numerous experiments, a numerical procedure with consideration of combination of upper bound theorem and stochastic medium theory is applied to the optimal analysis of shallow-buried tunnel failure. With help of functional catastrophe theory, this work presented a more accurate and optimal failure profile compared with previous work. Lastly the note discusses different effects of parameters in new yield rule and soil mechanical coefficients on failure mechanisms. The scope of failure block becomes smaller with increase of the parameter A and the range of failure soil mass tends to decrease with decrease of unit weight of the soil and tunnel radius, which verifies the geomechanics and practical case in engineering.

Keywords: optimization; shallow tunnels; functional catastrophe theory; settlement effect

1. Introduction

With the rapid development of the cities, more and more shallow-buried tunnels are constructing in urban areas. In practical engineering, it always occurs surface settlement during the process of the tunneling excavation. Furthermore, since the geomechanical properties of surrounding soil mass are very complicated, the tunnels are always bedded within many soil layers. So the effects of stochastic settlement on catastrophe failure modes of tunnel roof in different soil layers should be taken into account in research. By considering the nonlinear mechanical characteristics of geotechnical material in geomechanics and engineering, the linear model used to evaluate the stability of the tunnels and other geotechnical engineering has been replaced by the nonlinear modelling (Li and Yang 2017, 2018a, b, Mollon *et al.* 2011, Zhu *et al.* 2014).

Based on the stochastic medium theory, put forward by Litwiniszyn (1975), the movement of soil mass equals the sum of movement of stochastic medium elements induced by tunnel excavation. The ground surface settlement and transformation can be predicted considering the construction factors and formation conditions within this theory. Fang *et al.* (1994) made an estimation of ground settlement due to shield tunneling by the Peck-Fujita method. Fahimifar *et al.* (2015) predicted the ground response curve of underwater tunnels in strain-softening rock mass.

Due to the complexity and diversity of the constitutive relation of the engineering soils, many researchers put forward different yield rules to describe the mechanical behaviors of the soils. Hoek and Brown (1997) put forward a comprehensive description to calculate different mechanical properties of hard engineering soils, especially rocks. Based on the study of rocks, Liu *et al.* (2015) worked out the surrounding rock pressure of shallow-buried bilateral bias tunnels under earthquake. Qin *et al.* (2017) proposed two-dimensional and three-dimensional limit analysis of progressive collapse mechanism with help of Hoek-Brown failure criterion. Then Mohammadi *et al.* (2015) compared the generalized Hoek-Brown and Mohr-Coulomb failure criteria for stress analysis on the rocks failure plane. On the basis of previous research about nonlinear mechanical behaviors of engineering soils, Lee (2016) calculated the determination of tunnel support pressure under the pile tip using upper and lower bounds with a superimposed approach. Then Anyaegbunam (2015) made a rich synthesis about a generalized nonlinear power-type failure laws for geomaterials and this failure criterion is applied widely in the research of geotechnical engineering.

Because of the fact that the geomechanical changes in elastic and plastic materials are very complex and hard to predict during the process of the tunnel excavation, it is difficult to describe this process with the method of classical mathematical method. Thom (1975) proposed the catastrophe theory, of which the total potential is employed

*Corresponding author, Professor
E-mail: yangky@aliyun.com
[a]M.Sc. Student
E-mail: 526086057@qq.com

ISSN: 2005-307X (Print), 2092-6219 (Online)

in the form of a function. And quite a lot of practical problems were successfully solved in the catastrophe theory framework. On the basis of the previous literature reviews which focus on failure analysis of the tunnel roof without considering stochastic settlement and catastrophic failure during the tunneling, a new passive-active curved failure mechanism of shallow tunnel in layered soils is put forward. By making reference to the simple form non-linear failure criteria based on numerous experiments, a comprehensive and optimal solution for failure mechanisms in shallow-buried tunnels with stochastic settlement is presented with help of functional catastrophe theory. Furthermore a numerical procedure with combination of upper bound theorem and variational calculus is applied to the optimal analysis of passive and active failure of shallow tunnels, which describes mechanisms in which the self-weight of the soil, respectively, resists or assists failure. Then this work described a more accurate and optimal failure profile (experimental based) compared with previous work. Lastly this note investigated the effects of surface settlements and different geo-mechanical behaviors in different soil layers on the failure blocks.

2. Simplified stochastic medium theory and functional catastrophe theorem

2.1 Stochastic medium theory

For element system, soil mass corresponds to the global coordinate (x ,y ,z), while the excavation adopts the local coordinate (ξ,ζ,η). The dimensions of elemental excavation is defined as $d\xi$, $d\zeta$ and $d\eta$. The basic formulae for developing the equations for ground surface movement due to tunneling could be obtained. Fig. 1(a) shows an elemental excavation with dual coordinate systems. The preceding formulation is applicable to circular tunnel for equation derivation, as shown in Fig. 1(b). Assuming that every element failure completely in the whole excavation zone Ω, the ground surface settlement can be obtained by applying superposition principle, which can be written as

$$W_{\Omega}(x)=\iint_{\Omega}\frac{\tan\beta}{\eta}\exp\left[-\frac{\pi\tan^2\beta}{\eta^2}(x-\xi)^2\right]\mathrm{d}\xi\mathrm{d}\eta \tag{1}$$

where $W(x)$ is the ground surface settlement and β is the influence angle of ground settlement. Supposing that Ω is the initial cross section of tunnel, ω is the cross section after shrinkage and the radial convergence is $\Delta A_0=\Omega-\omega$, the ground surface settlement can be written as

$$W(x)=W_{\Omega}(x)-W_{\omega}(x)=\iint_{\Omega-\omega}\frac{\tan\beta}{\eta}\exp\left[-\frac{\pi\tan^2\beta}{\eta^2}(x-\xi)^2\right]\mathrm{d}\xi\mathrm{d}\eta \tag{2}$$

Then, the movement of ground surface can be obtained when the parameters β and ΔA_0 are determined. The horizontal displacement of ground surface, the differential surface settlement and the curvature of surface settlement profile can also be obtained.

2.2 Simplified stochastic surface settlement prediction

The stochastic medium theory is simplified, and the simplified ground surface settlement functions can be expressed as follows: The total ground surface settlement for the uniform convergence displacement mode can be written as

$$W(x)\approx\frac{2\pi R\Delta A_0\tan\beta}{H}\exp\left[-\frac{\pi\tan^2\beta}{H^2}x^2\right] \tag{3}$$

in which ΔA_0 is the radial convergence. The total ground surface settlement for the non-uniform convergence displacement mode is expressed as

$$W(x)\approx\frac{\pi Rg\tan\beta}{H}\exp\left[-\frac{\pi\tan^2\beta}{H^2}x^2\right] \tag{4}$$

where g is the gap parameter, and it is satisfied that $g=2\Delta A_0$. H is the distance between ground surface and the center of tunnel. In this work it is assumed that the ground surface settlement for the uniform convergence displacement mode is the same as the settlement for the non-uniform convergence displacement mode. The settlement curves corresponding to H=5 m, ΔA_0=60 mm and tanβ=1 with tunnel radius R varying from 5 m to 9 m are plotted, as shown in Fig. 1(c). It can be observed that the scope of ground settlement increase with the increase of tunnel radius. Since the scope of ground settlement is relatively small in practical engineering, the assumption that the settlement occurs in single layer is reasonable in this work.

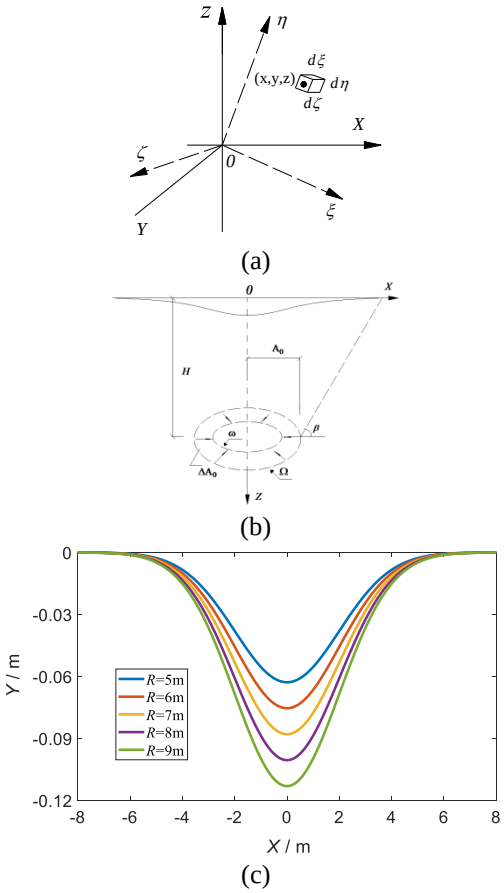

Fig. 1 (a) Ground movement in different systems, (b) Circular tunnel with stochastic settlement and (c) Stochastic settlement profile prediction with varying tunnel radius R

2.3 Functional catastrophe theory

Among a large number of nonlinear optimization theories used in geomechanics and engineering, the functional catastrophe theory put forward by Du (1994), has been developed in a quick pace and applied in many research fields, especially in complex nonlinear dynamic systems. Compared with other theories, the functional catastrophe theory is a better choice because of following reasons: (1) The mechanics of the conversion from continuous gradient to stable state in nonlinear dynamic system could be described by functional catastrophe theory more directly. (2) The quantitative state of the system can be predicted with a small number of control variables even without considering the constitutive equation and the mechanical properties of the soil mass system.

In the FCT, with help of analyzing the first- and second-order variations of the total potential, the degenerate critical point of the total potential could be obtained. Define the potential function of the system as $\left[V = f(x_1, x_2)\right]$, as in Eq. (5), and consider

$$J\left[f(x)\right] = \int_{x_1}^{x_2} F[f(x), f'(x), x]dx \tag{5}$$

in which a dot denotes a prime with respect to x, $f'(x) = \partial f(x)/\partial x$.

For the sake of getting the non-Morse critical point $f_c(x)$ of the potential function of the system, it is necessary to expand the increment of function to the forms of a two-variable Taylor series in small perturbations of y. This work makes $\left[y' = f'(x),\ y = f(x)\right]$ facilitate the derivation

$$\begin{aligned}\Delta J &= J[y+\delta y] - J(y)\\ &= \int_{x_1}^{x_2}\left[F(y+\delta y, y'+\delta y', x) - F(y, y', x)\right]dx\\ &= \int_{x_1}^{x_2}\left\{\left[\frac{\partial F}{\partial y}\delta y + \frac{\partial F}{\partial y'}\delta y'\right] + \frac{1}{2!}\left[\frac{\partial^2 F}{\partial y^2}\delta y^2 + 2\frac{\partial^2 F}{\partial y \partial y'}\delta y \partial y' + \frac{\partial^2 F}{\partial y'^2}\delta y'^2\right]\right.\\ &\quad \left. + \frac{1}{3!}\left[\frac{\partial^3 F}{\partial y^3}\delta y^3 + 3\frac{\partial^3 F}{\partial y^2 \partial y'}\delta y^2 \partial y' + 3\frac{\partial^3 F}{\partial y \partial y'^2}\delta y \partial y'^2 + \frac{\partial^3 F}{\partial y'^3}\delta y'^3\right] + \cdots\right\}dx\end{aligned} \tag{6}$$

Especially, the function F should reach the catastrophic point and J should reach the catastrophic point at the same time. The function F has a non-Morse critical point when it satisfies the following conditions

$$\begin{aligned} Df &= 0,\\ \det(Hf) &= 0,\end{aligned} \tag{7}$$

where Df and $\det(Hf)$ stand for the gradient and determinant of the Hesse matrix of potential function $f(x_1,x_2)$, respectively. According to Eq. (7), the conditions of function $J[y]$ are illustrated below

$$\begin{aligned}\delta J &= \int_{x_1}^{x_2}\left[\frac{\partial F}{\partial y}\delta y + \frac{\partial F}{\partial y'}\delta y'\right]dx\\ &= \int_{x_1}^{x_2}\left\{\begin{bmatrix}\frac{\partial F}{\partial y} & \frac{\partial F}{\partial y'}\end{bmatrix}\begin{bmatrix}\delta y\\ \delta y'\end{bmatrix}\right\}dx = 0,\end{aligned}$$

$$\begin{aligned}\delta J &= \int_{x_1}^{x_2}\left[\frac{\partial^2 F}{\partial y^2}\delta y^2 + 2\frac{\partial^2 F}{\partial y \partial y'}\delta y \partial y' + \frac{\partial^2 F}{\partial y'^2}\delta y'^2\right]dx\\ &= \int_{x_1}^{x_2}\left\{\begin{bmatrix}\delta y & \delta y'\end{bmatrix}\begin{bmatrix}\frac{\partial^2 F}{\partial y^2} & \frac{\partial^2 F}{\partial y \partial y'}\\ \frac{\partial^2 F}{\partial y \partial y'} & \frac{\partial^2 F}{\partial y'^2}\end{bmatrix}\begin{bmatrix}\delta y\\ \delta y'\end{bmatrix}\right\}dx = 0\end{aligned} \tag{8}$$

The form of catastrophic conditions of function $J[y]$ is illustrated in the following

$$\frac{\partial^2 \Lambda}{\partial f(x)^2} - 2\frac{\partial}{\partial x}\left(\frac{\partial^2 \Lambda}{\partial f(x)\partial f'(x)}\right) + \frac{\partial^2}{\partial x^2}\left(\frac{\partial^2 \Lambda}{\partial f'(x)^2}\right) = 0 \tag{9}$$

In this study, the detaching zone of a failure soil block is the studied system. Referring to the NL yield condition, the FCT is used to explore the optimization of failure mechanisms of shallow-buried tunnel with regard of stochastic settlement.

3. Failure mechanism analysis on the basis of nonlinear failure criterion

3.1 Simple form of Power-type yield rule

For simplicity, a power-type constitution of nonlinear soils is used by many publications to explore the mechanical behaviors of soils. Based on the previous work (Baker 2004, Li *et al*. 2017, Xu *et al*. 2018a, b, Xu and Yang 2018, Yang and Li 2018a, b, c, Yang *et al*. 2017, 2018), for the purpose of getting more optimal solutions, the present work employs a slight generalization of this nonlinear relation expressed as

$$\tau_n = P_a A\left(\frac{\sigma_n}{P_a} + T\right)^n \tag{10}$$

where τ_n and σ_n are shear and normal stress, respectively. P_a stands for atmospheric pressure; $\{A,n,T\}$= nondimensional strength parameters.

In particular, A is a scale parameter controlling the magnitude of shear strength, $\sigma_t=P_aT$ is the tensile strength, which T represents a non-dimensional tensile strength and shifts parameter controlling the location of the envelope on the σ axis, n controls the curvature of the envelope.

3.2 Nonlinear failure analysis with stochastic settlement

The supporting systems play a key role in the tunnel excavation in engineering. And the catastrophic failure

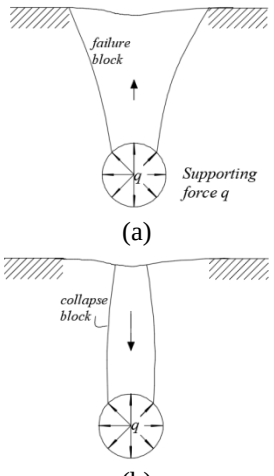

Fig. 2 Failure mechanism description for shallow tunnels, (a) passive mode and (b) active mode

often occurs during the supporting protection is used. If the applied force on tunnel roof is not big enough it will occur the surrounding soils move downwards to cause tunnel roof collapse; in the contrast, if the supporting systems is too strong, the soil mass would move upwards to cause the failure. According to Fig. 2, shallow circular tunnel is embedded within ideally plastic soil and the supporting pressure is defined as q. During the excavation of the tunneling surface settlement is not ignored and it has a significant influence on failure mode of the shallow tunnel. The rigid failure block is defined as active for downwards displacement, and passive for upwards displacement.

4. Catastrophe analysis of the shallow tunnel failure in layered soils

For simplicity, this work only illustrated the shallow tunnels embedded in two soil layers. However, this method can also be extended to solve the failure mechanisms of shallow tunnels embedded in several soil layers. Since the scope of ground settlement is relatively small in practical engineering, the assumption that the settlement occurs in single layer is reasonable in this work. As shown in Fig. 3 and Fig. 4, it is assumed that the failure mechanism is symmetrical with respect to y-axis and the curve of failure block is smooth. In order to get the reasonable solutions to describe the geometric profile of the failure block, it is assumed that the rates of plastic deformation are obtained from the yield function. According to the theory of the upper bound in limit analysis, put forward by Chen (1975), in this section the internal work produced by the shear stress and normal stress along the detaching lines and external work should be obtained first of all. Then the profiles of failure mass are obtained by functional catastrophe theory and the variational approach with help of virtual work formulation.

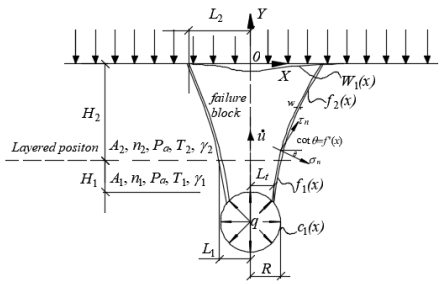

Fig. 3 Curved passive failure mechanism prediction for shallow tunnels with stochastic settlement

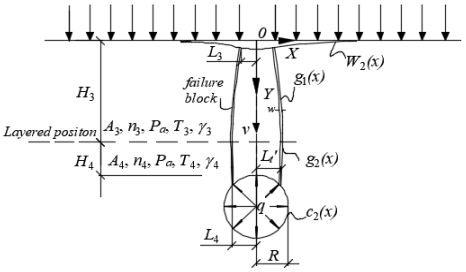

Fig. 4 Curved active failure mechanism prediction for shallow tunnels with stochastic settlement

4.1 Solution to characterize the failure shape in passive mechanism

The failure mechanism of shallow tunnel with stochastic settlement is different with deep tunnel due to its failure mode extending to the ground surface, as shown in Fig. 3.

The function $W_1(x)$ is the surface subsidence curve which is obtained using simplified stochastic medium theory, the curve of failure block is made up of two functions $f_1(x)$ and $f_2(x)$. H_1 is the height between the layered position and the top of tunnel and H_2 is the distance from ground surface to the layered position. Based on previous introduction, the expression of ground surface settlement curve is written as

$$W_1(x)=\frac{2\pi R\Delta A\tan\beta}{H_1+H_2+R}\exp\left[-\frac{\pi\tan^2\beta}{(H_1+H_2+R)^2}x^2\right] \tag{11}$$

Based on the previous work (Fraldi and Guarracino 2010, Yang 2018, Yang *et al*. 2017, Yang and Yao 2018, Yang and Zhang 2017), the energy dissipation density of any point on the detaching surface results are in Appendix

$$\begin{aligned}D&=\int_{L_t}^{L_1}\dot{D}_{f1}w\sqrt{1+f_1'(x)^2}\,\mathrm{d}x+\int_{L_t}^{L_2}\dot{D}_{f2}w\sqrt{1+f_2'(x)^2}\,\mathrm{d}x\\&=\int_{L_t}^{L_1}\left[-T_1+(1-n_1^{-1})(n_1A_1f_1'(x))^{\frac{1}{1-n_1}}\right]P_a\dot{u}\mathrm{d}x\\&+\int_{L_t}^{L_2}\left[-T_2+(1-n_2^{-1})(n_2A_2f_2'(x))^{\frac{1}{1-n_2}}\right]P_a\dot{u}\mathrm{d}x\end{aligned} \tag{12}$$

where L_1 stands for the failure width of upper and lower blocks, L_2 and L_t are the half-widths on the ground surface and the tunnel roof respectively. The 1 and 2 in the subscript of soil's parameters A, n, T and γ represent the lower soil and upper soil layers respectively. For the tunnel in layered soils, the work rate produced by self-weight is expressed as

$$W_e=\gamma_1\int_0^{L_t}c_1(x)\dot{u}\mathrm{d}x-\gamma_1\int_{L_t}^{L_1}f_1(x)\dot{u}\mathrm{d}x-\gamma_2\int_{L_t}^{L_2}f_2(x)\dot{u}\mathrm{d}x-\gamma_2\int_0^{L_2}W_1(x)\dot{u}\mathrm{d}x \tag{13}$$

where the expression of circular tunnel is written as follows

$$c_1(x)=-\left(H_1+H_2+R\right)+\sqrt{R^2-x^2} \tag{14}$$

As mentioned above, the failure mode of tunnel roof is determined by supporting structure. The work rate of supporting pressure q in the shallow circular tunnel is

$$W_q=Rq\dot{u}\arcsin\frac{L_t}{R} \tag{15}$$

Meanwhile, the work rate of extra force σ_s which puts on the ground surface in urban area cannot be ignored. The expressions can be written as

$$W_{\sigma_s}=-L_2\sigma_S\dot{u} \tag{16}$$

In order to obtain the upper bound solution, an objective function should be established using the energy dissipation and power of external forces, results

$$\begin{aligned}\Lambda&=D-W_e-W_q-W_{\sigma_s}\\&=\int_{L_t}^{L_1}\psi_1\left[f_1(x),f_1'(x),x\right]\dot{u}\mathrm{d}x+\int_{L_t}^{L_2}\psi_2\left[f_2(x),f_2'(x),x\right]\dot{u}\mathrm{d}x\\&-\gamma_1\int_0^{L_t}c_1(x)\dot{u}\mathrm{d}x+\gamma_2\int_0^{L_2}W_1(x)\dot{u}\mathrm{d}x-qR\arcsin\frac{L_t}{R}\dot{u}+\sigma_sL_2\dot{u}\end{aligned} \tag{17}$$

where

$$\int_{L_t}^{L_1}\psi_1\left[f_1(x),f_1'(x),x\right]\dot{u}\mathrm{d}x = \int_{L_t}^{L_1}\left[-T_1P_a+P_a(1-n_1^{-1})(n_1A_1f_1'(x))^{\frac{1}{1-n_1}}+\gamma_1f_1(x)\right]\dot{u}\mathrm{d}x \tag{18}$$

$$\int_{L_1}^{L_2}\psi_2\left[f_2(x),f_2'(x),x\right]\dot{u}\mathrm{d}x = \int_{L_1}^{L_2}\left[-T_2P_a+P_a(1-n_2^{-1})(n_2A_2f_2'(x))^{\frac{1}{1-n_2}}+\gamma_2f_2(x)\right]\dot{u}\mathrm{d}x \tag{19}$$

The problem also transforms into a typical calculus of variations, i.e., to find two functions, $y=f_1(x)$ and $y=f_2(x)$ when the extremum of objective function Λ is obtained. The extremum of objective function Λ can be obtained when the extreme values of two functions ψ_1 and ψ_2 are obtained simultaneously. According to variation principle, the Euler-Lagrange equations for the functions $\psi_1\left[f_1(x),f_1'(x),x\right]$ and $\psi_2\left[f_2(x),f_2'(x),x\right]$ result

$$\frac{\partial\psi_1}{\partial f_1(x)}-\frac{\partial}{\partial x}\left[\frac{\partial\psi_1}{\partial f_1'(x)}\right]=0\Leftrightarrow\gamma_1-P_a(n_1A_1)^{1/(1-n_1)}(n_1-1)^{-1}f_1'(x)^{(2n_1-1)/(1-n_1)}f_1''(x)=0 \tag{20}$$

$$\frac{\partial\psi_2}{\partial f_2(x)}-\frac{\partial}{\partial x}\left[\frac{\partial\psi_2}{\partial f_2'(x)}\right]=0\Leftrightarrow\gamma_2-P_a(n_2A_2)^{1/(1-n_2)}(n_2-1)^{-1}f_2'(x)^{(2n_2-1)/(1-n_2)}f_2''(x)=0 \tag{21}$$

The expressions of the detaching curve $f_1(x)$ and $f_2(x)$ are derived by integral calculation

$$f_1(x)=-k_1\left(\frac{a_1}{\gamma_1}-x\right)^{1/n_1}+a_2,\quad k_1=A_1^{-1/n_1}\left(\frac{\gamma_1}{P_a}\right)^{\frac{1-n_1}{n_1}} \tag{22}$$

$$f_2(x)=-k_2\left(\frac{a_3}{\gamma_2}-x\right)^{1/n_2}+a_4,\quad k_2=A_2^{-1/n_2}\left(\frac{\gamma_2}{P_a}\right)^{\frac{1-n_2}{n_2}} \tag{23}$$

where a_1, a_2, a_3 and a_4 being constants determined by boundary conditions. A geometrical relationship can be found from Fig. 3(a), that is

$$f_2(x=L_2)=W_1(x=L_2) \tag{24}$$

As there is also no distribution of shear stress on the ground surface, the following equation is obtained

$$\tau_{xy}(x=L_2,y=W_1(L_2))=0 \tag{25}$$

The expressions of a_3 and a_4 can be determined, $a_3=\rho_2L_2$ and $a_4=W_1(L_2)$. Thus, the expression of failure block in upper soil can be written as follows

$$f_2(x)=-k_2\left(L_2-x\right)^{1/n_2}+W_1(L_2) \tag{26}$$

When the curve of collapse block is smooth, the equations, $f_1'(x=L_1)=f_2'(x=L_1)$ should be satisfied. Another geometrical relationship $f_1(x=L_1)=-H_2$ can also be found from Fig. 3(a). Thus, the expressions of a_1 and a_2 can be obtained, $a_1=\gamma_1(L_1+Z_1)$ and $a_2=-H_2+k_1Z_1^{\frac{1}{n_1}}$ in which

$$Z_1=\left(\frac{n_1k_2}{n_2k_1}\right)^{\frac{n_1}{1-n_1}}\left(L_2-L_1\right)^{\frac{(n_2-1)n_1}{(n_1-1)n_2}} \tag{27}$$

The function of failure block in lower soil results

$$f_1(x)=-k_1\left(L_1+Z_1-x\right)^{\frac{1}{n_1}}-H_2+k_1Z_1^{\frac{1}{n_1}} \tag{28}$$

In order to get the upper bound solution, an equation can be obtained by equating the internal energy dissipation to the external work rate, let the function Λ equal zero

$$\begin{aligned}\Lambda=\dot{u}\Bigg\{&\left[-T_1P_a-\gamma_1H_2+\gamma_1k_1Z_1^{\frac{1}{n_1}}\right](L_1-L_t)+\left[\lambda_2W_1(L_2)-T_2P_a\right](L_2-L_1)\\&+\frac{n_1}{n_1+1}\left[P_a(1-n_1^{-1})(k_1A_1)^{\frac{1}{1-n_1}}-\gamma_1k_1\right]\cdot\left[(L_1+Z_1-L_t)^{\frac{n_1+1}{n_1}}-Z_1^{\frac{n_1+1}{n_1}}\right]\\&+\frac{n_2}{n_2+1}\left[P_a(1-n_2^{-1})(k_2A_2)^{\frac{1}{1-n_2}}-\gamma_2k_2\right]\cdot(L_2-L_1)^{\frac{n_2+1}{n_2}}-Rq\arcsin\frac{L_t}{R}\\&+(H_1+H_2+R)L_t+\frac{R^2}{2}\left[\arccos\frac{L_t}{R}-\frac{\pi}{2}-\frac{L_t}{R^2}\sqrt{R^2-L_t^2}\right]+\gamma_2\int_0^{L_2}W_1(x)\mathrm{d}x+L_2\sigma_S\Bigg\}\end{aligned} \tag{29}$$

According to Fig. 3, two geometrical conditions are still left, which can be expressed as

$$f_1(x=L_t)=c_1(x=L_t) \tag{30}$$

$$f_2\left(x=L_1\right)=-H_2 \tag{31}$$

Incorporating Eqs. (30) and (31) into Eq.(29), the values of L_1, L_2 and L_t can be solved by using numerical software. The integral $\int_0^{L_2}W_1(x)\mathrm{d}x$ in Eq. (17) cannot also be integrated for the simplest form, so the numerical solution of this integral is also calculated, and is substituted into the system of equation. Based on L_1, L_2 and L_t, the final forms of detaching curves $f_1(x)$ and $f_2(x)$ are obtained.

During the process of the catastrophe analysis of the stability of a shallow tunnel, the specific expressions of $f_1(x)$ and $f_2(x)$ can be obtained by substituting Eqs. (26) and (28) into Eq.(9), the results can be written as follows

$$A_i^{1/n_i}\gamma_i^{(2n_i-1)/n_i}P_a^{(1-n_i)/n_i}\left[\left(2n_i-1\right)\right]\left(\frac{a_{2i-1}}{\gamma_i}-x\right)^{-1/n_i}=0 \tag{32}$$

where i=1,2. Given any values of x, the Eq. (32) must be satisfied. Therefore, the value of n_i in Eq. (32) must be 0.5.

In previous work the form of the Hoek-Brown yield rule used by Fraldi and Guarracino (2010) was derived without using the notion of Mohr envelopes. This work makes the failure mechanism described more accurately and optimal since the extensive literature dealing with power-type criterion does not include the requirement $n\geq1/2$. According to Baker (2004), if $n<1/2$, the $S_{NL}(\sigma)$ intersects twice with the same Mohr circle. Therefore it is necessary to impose the restrictions $\{A>0,1/2\leq n\leq1,T\geq0\}$, because the radius of curvature of $S_{NL}(\sigma)$ is less than the radius of the tangential Mohr circle (Jiang *et al*. 2003) when $n<1/2$. This restrictions is satisfied in applications of this criterion to real experimental data (Hoek *et al.* 1980).

4.2 Analogous derivation for the collapsing shape in active mechanism

Similar with the passive failure mode, the active failure mechanism of tunnel roof can be considered with settlement curve $W_2(x)$ and analyzed by a new geometric profile, as

shown in Fig. 4. The curve of collapsing block is made up of two functions $g_1(x)$ and $g_2(x)$. H_3 and H_4 are the distances from ground surface to the layered position and the layered position to the top of tunnel, respectively.

$$W_2(x)=\frac{2\pi R\Delta A\tan\beta}{H_3+H_4+R}\exp\left[-\frac{\pi\tan^2\beta}{(H_3+H_4+R)^2}x^2\right] \tag{33}$$

In order to obtain the expression of objective function in active mode, by both considering supporting force and surcharge load, Eq.(17) takes the form

$$\Lambda=\int_{L_3}^{L_4}\psi_3[g_1(x),g_1'(x),x]vdx+\int_{L_4}^{L_t'}\psi_4[g_2(x),g_2'(x),x]vdx+\gamma_4\int_0^{L_t'}c_2(x)vdx -L_3\sigma_s v+Rqv\arcsin\frac{L_t'}{R} \tag{34}$$

in which

$$\begin{aligned}\psi_3[g_1(x),g_1'(x),x]&=-T_3P_a+P_a(1-n_3^{-1})(n_3A_3g_1'(x))^{\frac{1}{1-n_3}}-\gamma_3g_1(x)\\ \psi_4[g_2(x),g_2'(x),x]&=-T_4P_a+P_a(1-n_4^{-1})(n_4A_4g_2'(x))^{\frac{1}{1-n_4}}-\gamma_4g_2(x)\\ c_2(x)&=(H_3+H_4+R)-\sqrt{R^2-x^2}\end{aligned} \tag{35}$$

L_4 stands for the collapsing width of upper and lower blocks, L_3 and L'_t are the half-widths on the ground surface and the tunnel roof respectively. The 3 and 4 in the subscript of soil's parameters A, n, T and γ represent the upper soil and lower soil layers, respectively.

As shown in Fig. 4, the explicit expressions of the function of velocity discontinuity surface should fulfill other boundary conditions. Such as

$$\begin{aligned}\tau_{xy}(x=L_3,y=W_2(L_3))&=0\\ W_2(x=L_3)&=g_1(x=L_3)\\ g_1'(x=L_4)&=g_2'(x=L_4)\\ g_2(x=L_4)&=H_3\end{aligned} \tag{36}$$

$$\begin{aligned}g_1(x=L_4)&=H_3\\ c_2(x=L_t')&=g_2(x=L_t')\end{aligned} \tag{37}$$

As the same with passive failure mechanism, also by the calculus of variations, the mathematical expression of failure surface in active failure mode takes the form below

$$\begin{aligned}g_1(x)&=k_3(x-L_3)^{\frac{1}{n_3}}+W_2(L_3)\\ g_2(x)&=k_2(x-L_4+Z_2)^{\frac{1}{n_4}}+H_3-k_4Z_2^{\frac{1}{n_4}}\end{aligned} \tag{38}$$

in which

$$\begin{aligned}Z_2&=\left(\frac{n_4k_3}{n_3k_4}\right)^{\frac{n_4}{1-n_4}}(L_4-L_3)^{\frac{(n_3-1)n_4}{(n_4-1)n_3}}\\ k_3&=A_3^{-1/n_3}\left(\frac{\gamma_3}{P_a}\right)^{\frac{1-n_3}{n_3}}\\ k_4&=A_4^{-1/n_4}\left(\frac{\gamma_4}{P_a}\right)^{\frac{1-n_4}{n_4}}\end{aligned} \tag{39}$$

Incorporating Eq. (37) into equation Λ=0, the values of L_3, L_4 and L'_t can be solved by using numerical software. Based on L_3, L_4 and L'_t, the final forms of detaching curves $g_1(x)$ and $g_2(x)$ are obtained. Also by catastrophe theory n_3 and n_4 should be 0.5 synchronously. Especially when L_3=0, the critical height H_{cr} which distinguishes the deep and shallow tunnel could be obtained. Therefore it is assumed that this failure mechanism should satisfy the condition $H_3+H_4\le H_{cr}$.

Table 1 Comparisons between existing upper-bound solutions and this results

Frictional angle ϕ'(°)	Upper bound solution (Smith 1998)	Upper bound solution (this paper)
25	0.4650	0.4663
30	0.5754	0.5774
35	0.6974	0.7002
40	0.8349	0.8391
45	0.9940	1.0000
50	1.1831	1.1918

Table 2 Comparisons in upper bound solutions of the size of the collapsing blocks of shallow tunnel

n	H_1	H_2	A_1	A_2	γ_1	Γ_2	L_1 (This work)	L_1 (Yang's work)
	m	m			kN/m^3	kN/m^3	m	m
0.5	3	2	0.9	0.8	16	16	1.7242	1.7677
0.5	3	2	0.8	0.7	16	16	2.1192	2.1213
0.5	3	2	0.7	0.6	16	16	2.4190	2.4748
0.5	3	2	0.6	0.5	16	16	2.7320	2.8284
0.5	3	2	0.75	0.75	20	19	2.6231	2.6516
0.5	3	2	0.75	0.75	19	18	2.5190	2.5724
0.5	3	2	0.75	0.75	18	17	2.4288	2.5000
0.5	3	2	0.75	0.75	17	16	2.3072	2.4333

5. Sensitivity analysis and discussions

In order to investigate the effects of different parameters on failure mechanism of shallow circular tunnel in layered soils, the explicit failure surfaces around circular tunnel crown should be plotted and compared with different values. In general, with considering different underground water levels, the deeper the depth of the tunnel buries, the better the nature of the hard soil mass is. So with the increase of the buried depth, the parameter A and unit self-weight will become larger. For the purpose of making comparisons with existing work, let r_u=0 and m=1, good agreement is shown in passive and active mode for shallow tunnel, as shown in Table 1.

(1)The influence of parameter A on failure mechanism in layered soils

According to the Fig. 5, the failure profile of tunnel roof with different values of A are obtained corresponding $n_i(i=1,2,3,4)=0.5$, $\gamma_i(i=1,2,3,4)=18$ kN/m^3, $T_i(t=1,2,3,4)=0.25$, P_a=100 kPa, R=5 m, H_1=H_4=3 m and H_2=H_3=2 m. Based on the practical engineering experience, the parameters are ΔA_0=2.5 mm and tanβ=1 in passive mode, as shown in Fig. 5(a), the failure mode calculated in this work is very similar with previous work (Yang and zhang 2018), the comparisons in upper bound failure size are made, as shown in Table 2; also let ΔA_0=1.5 mm and

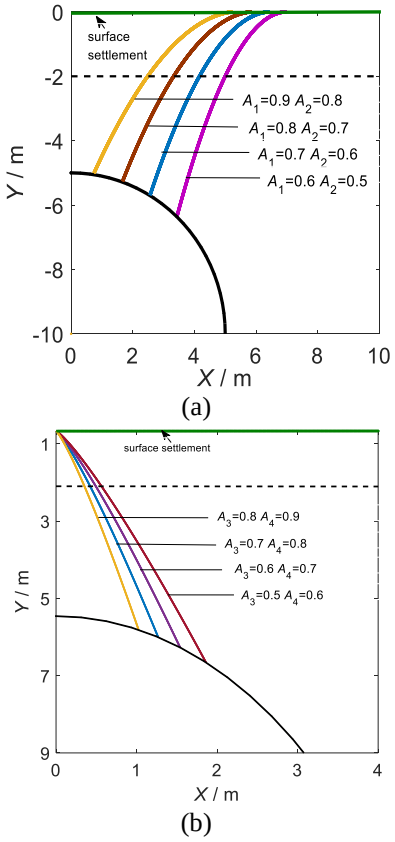

Fig. 5 Effects of parameter A on failure mechanisms of shallow circular tunnel, (a) passive mode and (b) active mode

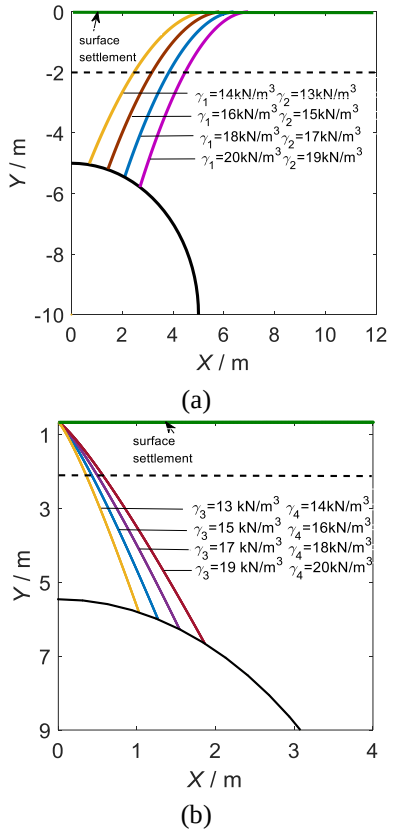

Fig. 6 Effects of soil unit weight on failure mechanisms of shallow tunnel, (a) passive mode and (b) active mode

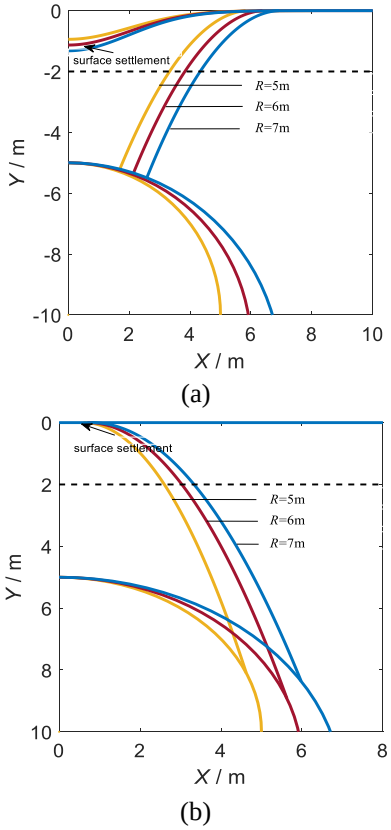

Fig. 7 Effects of tunnel radius R on failure mechanisms of shallow circular tunnel, (a) passive mode and (b) active mode

tanβ=0.5 in active mode, as shown in Fig. 5(b), the shapes of the collapse blocks presented in this paper when q=0 and L_3=0 are almost equal to those calculated by Fraldi and Guarracino (2010). As mentioned above, when the supporting force q is very small (even to zero), it would occur the active failure for the tunnel crown; however, when the supporting force q is very big, the passive catastrophe failure will happen. So in his work q=0 MPa for the active mode in the shallow circular tunnel, while q=0.4 MPa for the passive mode. It could be concluded that the failure modes and the derivation put forward in this note are valid because of good agreement with previous work. From the standpoint of geomechanics, with the increase of A the size of the potential failure blocks decreases. From the perspective of engineering, supporting system for shallow tunnel should be intensified when the parameter A is small.

(2) The influence of unit weight γ on failure mechanism in layered soils

According to the Fig. 6, the failure profile of tunnel roof with different values of γ are obtained corresponding n_i(i=1,2,3,4)=0.5, A_i(i=1,2,3,4)=0.8, T_i(i=1,2,3,4,)=0.25, P_a=100 kPa R=5 m, H_1=H_4=3 m and H_2=H_3=2 m. As mentioned above, the parameters are ΔA_0=2.5 mm and tanβ=1 in passive mode, the comparisons in upper bound failure size are made, as shown in Table 2; ΔA_0=1.5 mm and tanβ=0.5 in active mode. q = 0 MPa for the active mode in the shallow circular tunnel, while q=0.4 MPa for the passive mode. And the passive-active failure modes also agree well with previous work. With the increase of γ the scope of the potential failure blocks becomes larger. From the

perspective of engineering, supporting system for shallow tunnel should be intensified when the unit weight γ is big enough.

(3) The influence of tunnel radius R on failure mechanism in layered soils

According to the Fig. 7, the failure profile of tunnel roof with different values of R are obtained corresponding $n_i(i=1,2,3,4)=0.5$ $A_i(i=1,2,3,4)=0.8$, $\gamma_i(i=1,2,3,4)=18$ kN/m^3, $T_i(t=1,2,3,4)=0.25$, $P_a=100$ kPa, $H_1=H_4=3$ m and $H_2=H_3=2$ m.. In order to make comparisons clearly and plot figures easily, the parameters are $\Delta A_0=150$ mm and $\tan\beta=1$ in passive mode; $\Delta A_0=1.5$ mm and $\tan\beta=0.5$ in active mode. With the increase of R the scope of the potential failure blocks becomes larger. From the perspective of engineering, supporting system for shallow tunnel should be intensified when the unit weight R is big enough.

6. Conclusions

On the basis of previous work which has focused the efforts on the collapse mechanism without considering combined influence of stochastic settlement and nonlinear optimization approach during the tunneling, a new passive-active curved failure mechanism of shallow tunnel in layered soils is put forward. This work explored the influences of surfaces settlement and different geo-mechanical behaviors in different soil layers on the failure blocks. By making reference to the simple form non-linear failure criteria based on numerous experiments, a comprehensive and optimal solution for failure mechanisms in shallow circular tunnels with stochastic settlement is presented with help of functional catastrophe theory. Some conclusions are drawn from above:

(1) A numerical procedure with combination of upper bound theorem and variational calculus is applied to the analysis of active and passive failure of shallow tunnels with stochastic settlement for a power-type (experimental based) material yield rule.

(2) This work makes the failure mechanism described more accurately and optimal compared with previous work dealing with power-law criterion which does not include the requirement $n\geq 1/2$. This requirement is satisfied in applications of this criterion to real experimental data.

(3) This note investigates different effects of different parameters in simple nonlinear yield criterion and soil mechanical parameters on the possible failure scope of shallow tunnel. The range of failure soil mass tends to decrease with decrease of unit weight of the soil and tunnel radius. On the contrast, the scope of failure block becomes smaller with increase of the parameter A, which verifies the geomechanics and practical case in engineering.

Acknowledgements

Financial support was received from National Natural Science Foundation (51378510) for the preparation of this manuscript. This financial support is greatly appreciated.

References

Anyaegbunam, A.J. (2015), "Nonlinear power-type failure laws for geomaterials: Synthesis from triaxial data, properties, and applications", *J. Geomech.*, **15**(1), 04014036.

Baker, R. (2004), "Nonlinear Mohr envelopes based on triaxial data", *J. Geotech. Geoenviron. Eng.*, **130**(5), 498-506.

Chen, W.F. (1975), *Limit Analysis and Soil Plasticity*, Elsevier Science, Amsterdam, The Netherlands.

Du, X.F. (1994), *Application of Catastrophe Theory in Economic Field*, Xi'an Electronic Science and Technology University Press, Chengdu, China.

Fahimifar, A., Ghadami, H. and Ahmadvand, M. (2015), "The ground response curve of underwater tunnels excavated in a strain-softening rock mass", *Geomech. Eng.*, **8**(3), 323-359.

Fang, Y.S., Lin, J.S. and Su, C.S. (1994), "An estimation of ground settlement due to shield tunneling by the Peck-Fujita method", *Can. Geotech. J.*, **31**(3), 431-443.

Fraldi, M. and Guarracino, F. (2010), "Analytical solutions for collapse mechanisms in tunnels with arbitrary cross sections", *J. Solid. Struct.*, **47**(2), 216-223.

Hoek, E. and Brown, E.T. (1980), *Underground Excavations in Rock*, CRC Press, Boca Raton, Florida, U.S.A., 1165-1186.

Hoek, E. and Brown, E.T. (1997), "Practical estimates of rock mass strength", *J. Rock Mech. Min. Sci.*, **34**(8), 1165-1186..

Jiang, J.C, Baker, R. and Yamagami, T. (2003), "The effect of strengthenvelope nonlinearity on slope stability computations," *Can. Geotech. J.*, **40**(2), 308-325.

Lee, Y.J. (2016), "Determination of tunnel support pressure under the pile tip using upper and lower bounds with a superimposed approach", *Geomech. Eng.*, **11**(4), 587-605.

Litwiniszyn, J. (1957), "The theories and model research of movements of ground masses", *Proceedings of the European Congress Ground Movement*, Leeds, U.K., April.

Li, T.Z., Li, Y.X. and Yang, X.L. (2017), "Rock burst prediction based on genetic algorithms and extreme learning machine", *J. Central South Univ.*, **24**(9), 2105-2113.

Li, T.Z. and Yang, X.L. (2017), "Limit analysis of failure mechanism of tunnel roof collapse considering variable detaching velocity along yield surface", *J. Rock Mech. Min. Sci.*, **100**, 229-237.

Li, T.Z. and Yang, X.L. (2018a), "Risk assessment model for water and mud inrush in deep and long tunnels based on normal grey cloud clustering method", *KSCE J. Civ. Eng.*, **22**(5), 1991-2001.

Li, T.Z. and Yang, X.L. (2018b), "Reliability analysis of tunnel face in broken soft rocks using improved response surface method", *J. Geomech.*, **18**(5), 04018021.

Liu, X.R., Li, D.L., Wang, J.B. and Wang, Z. (2015), "Surrounding rock pressure of shallow-buried bilateral bias tunnels under earthquake", *Geomech. Eng.*, **9**(4), 427-445.

Mohammadi, M. and Tavakoli, H. (2015), "Comparing the generalized Hoek-Brown and Mohr-Coulomb failure criteria for stress analysis on the rocks failure plane", *Geomech. Eng.*, **9**(1), 115-124.

Mollon, G., Dias, D. and Soubra, A.H. (2011), "Rotational failure mechanisms for the face stability analysis of tunnels driven by a pressurized shield", *J. Numer. Anal. Meth. Geomech.*, **35**(12), 1363-1388.

Qin, C.B., Chian, S.C. and Yang, X.L. (2017), "3D limit analysis of progressive collapse in partly weathered Hoek-Brown rock banks", *J. Geomech.*, **17**(7), 04017011.

Smith, C.C. (1998), "Limit loads for an anchor/trapdoor embedded in an assoviative coulomb soil", *J. Numer. Anal. Meth. Geomech.*, **22**(11), 855-865.

Thom, R. (1972), *Structural Stability and Morphogenesis*, Westview Press, Boulder, Colorado, U.S.A.

Xu, J.S., Li, Y.X. and Yang, X.L. (2018a), "Stability charts and reinforcement with piles in 3D nonhomogeneous and anisotropic soil slope", *Geomech. Eng.*, **14**(1), 71-81.

Xu, J.S., Pan, Q.J., Yang, X.L. and Li, W.T. (2018b), "Stability

charts for rock slopes subjected to water drawdown based on the modified nonlinear Hoek-Brown failure criterion", *J. Geomech.*, **18**(1), 04017133.

Xu, J.S. and Yang, X.L. (2018), "Effects of seismic force and pore water pressure on three dimensional slope stability in nonhomogeneous and anisotropic soil", *KSCE J. Civ. Eng.*, **22**(5), 1720-1729.

Yang, X.L. (2018), "Lower-bound analytical solution for bearing capacity factor using modified Hoek-Brown failure criterion", *Can. Geotech. J.*, **55**(4), 577-583.

Yang, X.L. and Li, Z.W. (2018a), "Kinematical analysis of 3D passive earth pressure with nonlinear yield criterion", *J. Numer. Anal. Meth. Geomech.*, **42**(7), 916-930.

Yang, X.L. and Li, Z.W. (2018b), "Upper bound analysis of 3D static and seismic active earth pressure", *Soil Dyn. Earthq. Eng.*, **108**, 18-28.

Yang, X.L. and Li, Z.W. (2018c), "Factor of safety of three-dimensional stepped slope", *J. Geomech.*, **18**(6), 04018036.

Yang, X.L., Li, Z.W., Liu, Z.A. and Xiao, H.B. (2017), "Collapse analysis of tunnel floor in karst area based on Hoek-Brown rock media", *J. Central South Univ.*, **24**(4), 957-966.

Yang, X.L. and Yao, C. (2018), "Stability of tunnel roof in nonhomogeneous soils", *J. Geomech.*, **18**(3), 06018002.

Yang, X.L. and Zhang, R. (2017), "Collapse analysis of shallow tunnel subjected to seepage in layered soils considering joined effects of settlement and dilation", *Geomech. Eng.*, **13**(2), 217-235.

Yang, X.L. and Zhang, R. (2018), "Limit analysis of stability of twin shallow tunnels considering surface settlement", *KSCE J. Civ. Eng.*, **22**(5), 1967-1977.

Yang, X.L., Zhou, T. and Li, W.T. (2018), "Reliability analysis of tunnel roof in layered Hoek-Brown rock masses", *Comput. Geotech.*

Yang, Z.H., Zhang, R., Xu, J.S. and Yang X.L. (2017), "Energy analysis of rock plug thickness in karst tunnels based on non-associated flow rule and nonlinear failure criterion", *J. Central South Univ.*, **24**(12), 2940-2950.

Zhu, H.H., Mei, G.X., Xu, M., Liu, Y. and Yin, J.H. (2014), "Experimental and numerical investigation of uplift behavior of umbrella-shaped ground anchor", *Geomech. Eng.*, **7**(2), 165-181.

CC

Appendix: Derivation of the dissipation density

By assuming the plastic potential, ξ, to be coincident with the Mohr envelope and considering without any loss of generality, τ_n is positive, it is

$$\xi = \tau_n - P_a A(\frac{\sigma_n}{P_a} + T)^n \tag{40}$$

So that the plastic strain rate can be written as follows

$$\begin{aligned} \dot{\varepsilon}_n &= \lambda \frac{\partial \xi}{\partial \sigma_n} = -\lambda n A(\frac{\sigma_n}{P_a} + T)^{(n-1)} \\ \dot{\gamma}_n &= \lambda \frac{\partial \xi}{\partial \tau_n} = \lambda \end{aligned} \tag{41}$$

where λ is a scalar parameter. The plastic strain rate components can be written in the form

$$\begin{aligned} \dot{\varepsilon}_n &= \frac{\dot{u}}{w}\left[1 + f'(x)^2\right]^{-\frac{1}{2}} \\ \dot{\gamma}_n &= -\frac{\dot{u}}{w} f'(x)\left[1 + f'(x)^2\right]^{-\frac{1}{2}} \end{aligned} \tag{42}$$

where w is the thickness of the plastic detaching zone. A dot denotes differentiation with respect to time, i.e., $\dot{u} = \partial u / \partial t$.

In order to enforce compatibility, from Eqs. (41) and (42) it follows

$$\lambda = -\frac{\dot{u}}{w} f'(x)\left[1 + f'(x)^2\right]^{-\frac{1}{2}} \tag{43}$$

and the normal component of stress can be written as

$$\sigma_n = \left[-T + (nAf'(x))^{\frac{1}{1-n}}\right] P_a \tag{44}$$

So that, by virtue of the Greenberg minimum principle, the effective collapse mechanism can be found by minimizing the total dissipation, the dissipation density of the internal forces on the detaching surface, $\dot{D}_i$, results

$$\dot{D}_i = \sigma_n \dot{\varepsilon}_n + \tau_n \dot{\gamma}_n = \left\{ P_a \cdot \left[-T + (1 - n^{-1})(nAf'(x))^{\frac{1}{1-n}}\right] \Big/ \left[w\sqrt{1 + f'(x)^2}\right] \right\} \dot{u} \tag{45}$$

where $\dot{\varepsilon}_n$ is normal plastic strain, $\dot{\gamma}_n$ is shear plastic strain rates, w is the thickness of the plastic detaching zone, and $\dot{u}$ is the velocity of the collapsing block.